Author statement

Giulia De Soricellis: Methodology, Investigation. **Francesco Fagnani**: Methodology, Investigation. **Alessia Colombo**: Conceptualization, Methodology, Writing- Original draft preparation ,Writing- Reviewing and Editing, Supervision **Claudia Dragonetti:** Conceptualization, Writing- Original draft preparation, Writing- Reviewing and Editing. **Dominique Roberto**: Resources, Writing- Original draft preparation, Writing- Reviewing and Editing. **Daniele Marinotto**: Investigation; Methodology Writing- Reviewing and Editing. **David H. Hartnell:** Methodology, Investigation. **Mark J. Hackett:** Methodology, Investigation. **Massimiliano Massi:** Conceptualization,Writing- Original draft preparation Supervision. **Bertrand Carboni**: Methodology, Supervision. **Véronique Guerchais:** Methodology, Resources

GA

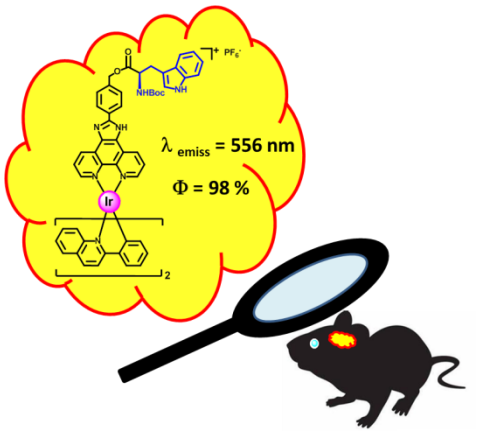

Cyclometalated Ir(III) dyes for neuroimaging applications

An attractive family of cyclometalated Ir(III) dyes functionalized with tryptophan for potential neuroimaging applications

Giulia De Soricellis, [‡, a] Francesco Fagnani, [‡, a] Alessia Colombo,*[a] Claudia Dragonetti,[a] Dominique Roberto,[a] Daniele Marinotto,[b] David H. Hartnell[c], Mark J. Hackett,[c] Massimiliano Massi[c], Bertrand Carboni,[d] and Véronique Guerchais[d]

[a.] Dipartimento di Chimica, Università degli Studi di Milano, UdR INSTM di Milano, via C. Golgi 19, 20133 Milan, Italy. alessia.colombo@unimi.it

[b] Istituto di Scienze e Tecnologie Chimiche (SCITEC) "Giulio Natta", Consiglio Nazionale delle Ricerche (CNR), via C. Golgi 19, 20133 Milan, Italy.

[c] School of Molecular and Life Sciences, Curtin University, Kent Street, Perth, Australia 6845.

[d] Université de Rennes 1, CNRS, ISCR (Institut des Sciences Chimiques de Rennes) - UMR 6226, F-35000 Rennes, France.

[‡] These authors have contributed equally to this work.

Abstract

Three novel luminescent iridium(III) dyes functionalized with a tryptophan amino acid and bearing two cyclometalated 2-phenylpyridines, 2-(2,4-difluorophenyl)pyridines or 2-phenylquinolines have been prepared and well characterized. They emit at 522-561 nm with a luminescence quantum yield in the range 0.33-0.98. All the dyes are able to stain neuronal cells in rat cerebellum tissue, as evidenced by fluorescence microscopy, showing affinity for granule neurons. The complexes bearing cyclometalated 2-(2,4-difluorophenyl)pyridines or 2-phenylquinolines also have a good affinity for brain white matter. The dye with two cyclometalated 2-phenylquinolines is characterized by the best luminescence quantum yield (0.98). Besides, giving the greatest image

contrast, the dye with two cyclometalated 2-phenylquinolines shows the strongest affinity for a distinct subtype of neurons found in cerebellum tissue, the purkinje neurons (as evidenced with fluorescence microscopy).

Keywords

Iridium dyes, cyclometalated iridium(III) phenanthroline complexes, phosphorescence, bio-imaging, optical markers, brain tissue staining

1. Introduction

Bis-cyclometalated phenylpyridine iridium(III) complexes are fascinating for their two-photon absorption activity [1-8] and for their second-order nonlinear optical [9-17] and luminescent [18-19] properties. In the last two decades, a lot of work has been devoted to the synthesis of various neutral and cationic bis-cyclometalated phenylpyridine iridium(III) complexes for many applications such as emissive materials for organic light emitting diodes (OLED) [20-27] and organic light-emitting electrochemical cells (OLEC) devices [20, 28-34], photoredox catalysis for visible light activated organic reactions [35-36] and polymerization processes [37-38], dye-sensitized solar cells [39-42], and luminescent solar concentrators [43]. Today, a field of increasing interest is their application as luminescent labels for bio-imaging and bio-sensing [44-48], and as tool in modern medicine and particularly in photodynamic therapy [46-48].

A key reason for the use of a heavy metal-containing compound as luminescent probe is that its emission decay lifetime is usually much longer than typical emission lifetimes of fluorescent organic molecules. Owing to the heavy metal atom, high spin-orbit coupling increases the rate of intersystem crossing, allowing the efficient population of excited triplet states and facilitating phosphorescence, thus expanding the emission lifetime scale towards the microseconds. Luminescent cyclometalated iridium(III) complexes have many advantages over the currently

available bio-imaging agents [46-48]. These include a good photochemical and chemical stability within the cellular environment, permeability, minimization of self-quenching due to the significant Stokes' shift, long-lived triplet excited state ($\tau \sim \mu s$) compared to organic dyes ($\tau \sim$ ns) that helps to eliminate the short-lived autofluorescence of biological samples, and microenvironment-sensitive emission characteristics which are less damaging to cellular components. The high photostability of these complexes allows the continuous monitoring of biological events by fluorescence spectroscopy and microscopy [46-48]. While a lot of effort has been devoted to the study of heavy metal complexes as cellular labels [49-52], the use of these complexes for the staining of tissue has comparatively received little attention.

A few years ago, it was reported that the bis-cyclometalated phenylpyridine iridium(III) complex bearing a (1H-imidazo[4,5-f][1,10]phenanthrolin-2-yl)benzene ligand is characterized by a good luminescence quantum yield (56%) and a long lifetime (0.66 μs) [53]. Following this work, we prepared and investigated related complexes functionalized with a tryptophan amino acid; the complexes present structural variations, in view of assessing how the modification would affect imaging properties (Chart 1). Tryptophan is the precursor of two significant biomolecules: serotonin and L-kynurenine [54] whose biosynthesis takes place in the brain, implying that tryptophan penetrates in the blood-brain-barrier (BBB) [55]. For this reason, we speculated the newly prepared complexes would be good candidates to investigate in brain tissue.

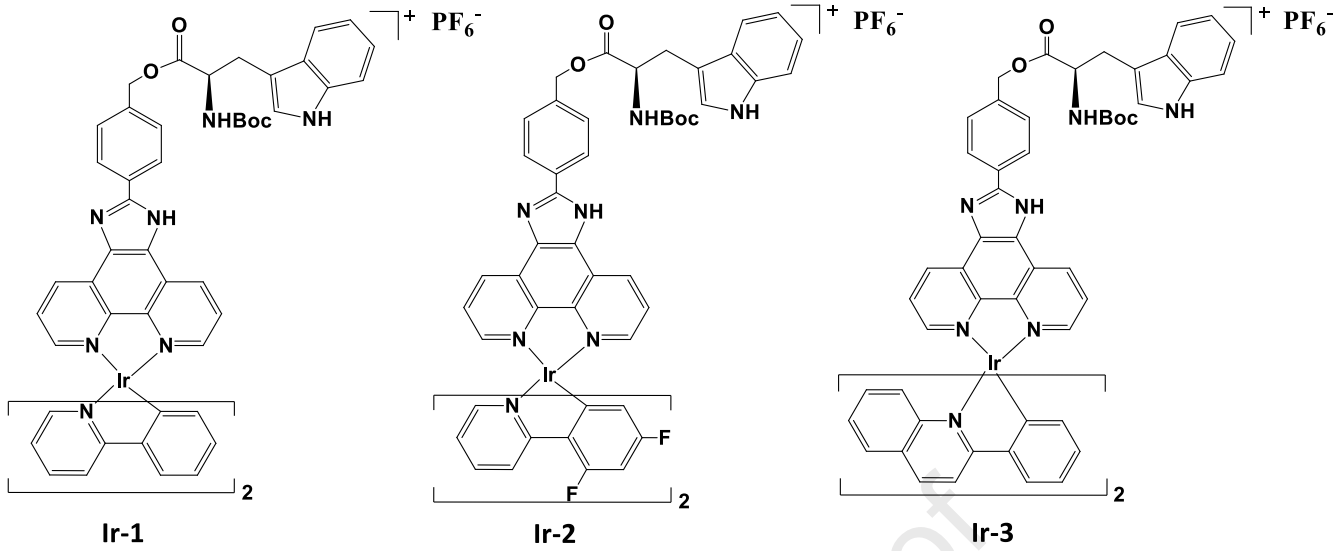

Chart 1. Structure of the investigated complexes.

2. Materials and Methods

2.1 General information

All the commercially available reagents were used as purchased without further treatments. Anhydrous solvents (MeOH, DMF) were subjected to prior distillation following the proper procedure reported in literature. Air- and water-sensitive reactions were performed in flame-dried glassware under argon atmosphere. Oxygen sensitive reaction were carried out vigorously bubbling argon into the solvent. ^{1}H NMR (300, 400 or 500 MHz), ^{13}C NMR (75, 101 or 126 MHz) and ^{19}F (376 MHz) spectra were recorded on Bruker AC 300 and AC 400 spectrometers. Chemical shifts δ are given in ppm and coupling constants J in Hz. Multiplicities are reported as indicated: s = singlet, d = doublet, t = triplet, q = quartet, m = multiplet, br = broad. High-resolution mass spectra (HRMS) were recorded, either on a Bruker MaXis 4G, an Agilent 6510, or a Thermo Fisher Q-Exactive spectrometer (Centre Régional de Mesures Physiques de l'Ouest, Rennes) using positive or negative ion Electron-Spray ionization techniques (respectively ESI+, ESI-). Purifications by silica gel chromatography were carried out on silica 0.060-0.200 mm, 60 A. Flash chromatography

were performed on a Grace Reveleris™ apparatus. Analytical thin layer chromatography was performed on Merck Silica Gel 60 F254 plates. Elemental analyses were performed by the Department of Chemistry of the University of Milan. *NMR spectra are in the* Supplementary material.

2.2 Synthesis of cyclometalated iridium complexes

*2.2.1 Synthesis of (R)-4-(1H-imidazo[4,5-f][1,10]phenanthrolin-2-yl)benzyl 2-((tert-butoxycarbonyl)amino)-3-(1H-indol-3-yl)propanoate (**L-trp**)*

The tryptophan functionalized phenanthroline ligand (**L-trp**) was prepared in two steps: (i) synthesis of (4-(1H-imidazo[4,5-f][1,10]phenanthrolin-2-yl)phenyl)methanol and (ii) functionalization with the tryptophan moiety.

2.2.1.1 Synthesis of the intermediate (4-(1H-imidazo[4,5-f][1,10]phenanthrolin-2-yl)phenyl)methanol

Under inert atmosphere, 1,10-phenanthroline-5,6-dione (0.24 g, 1.1 mmol), 4-(4-hydroxymethyl)benzaldehyde (0.18 g, 1.3 mmol), ammonium acetate (1.74 g, 22.5 mmol) and glacial acetic acid (4 mL) were placed in a Schlenk tube fitted with a condenser. The vessel was then sealed and heated under reflux for four hours. The mixture was cooled to room temperature and neutralized with aqueous ammonia. The lacquer deposited on the glassware was isolated and washed pouring water (10 mL) under sonication. A suspension was thus obtained. The yellow solid was filtered, washed with diethyl ether (15 mL) and dried under vacuum. The ^{1}H NMR spectrum exhibited the coexistence of (4-(1H-imidazo[4,5-f][1,10]phenanthrolin-2-yl)phenyl)methanol and the related acetic ester.

The yellow powder (388 mg) was thus solubilized in 5 mL of dry MeOH under Ar, subsequently adding 3 mL of a 30% solution of MeONa in MeOH in a dropwise manner. The mixture was let stir for three hours at room temperature. In the end, 1 mL of a saturated solution of NH_4Cl allowed the

precipitation of the desired product, which was isolated through filtration. The isolated yellow solid was washed with 5 mL of water, 10 mL of diethyl ether and dried under vacuum (200 mg). **Yield:** 54%. **^{1}H-NMR** (400 MHz, DMSO, δ): 9.04 (d, *J* = 3.8 Hz, 2H), 8.94 (d, *J* = 7.9 Hz, 2H), 8.27 (d, *J* = 8.0 Hz, 2H), 7.80-7.89 (m, 2H), 7.57 (d, *J* = 8.0 Hz, 2H), 5.34 (t, *J* = 5.6 Hz, 1H), 4.63 (d, *J* = 5.3 Hz, 2H).

2.2.1.2 (R)-4-(1H-imidazo[4,5-f][1,10]phenanthrolin-2-yl)benzyl 2-((tert-butoxycarbonyl)amino)-3-(1H-indol-3-yl)propanoate ***(L-Trp)***

In a Schlenk tube filled with Ar, Boc-protected tryptophan (0.47 g, 1.5 mmol), hydroxybenzotriazole (HOBt, 0.21 g, 1.5 mmol) and 1-ethyl-3-(3-dimethylaminopropyl)carbodiimide (EDC, 0.30 g, 1.5 mmol) were dissolved in 8 mL of dry DMF amine free at 0°C. The mixture was let stir for one hour after the addition of Et_3N (0.21 mL, 1.5 mmol). In the end, (4-(1H-imidazo[4,5-f][1,10]phenanthrolin-2-yl)phenyl)methanol (0.20 g, 0.6 mmol) was introduced before sealing the vessel and heating at 70°C for 72h. The solution was then cooled to room temperature and concentrated *in vacuo.* The crude product was purified through silica gel flash chromatography, using a mixture of dichloromethane:methanol, 19:1, v/v, as the eluent. The desired compound, **L-trp**, was obtained as a yellow solid (266 mg). **Yield:** 69% . **^{1}H-NMR** (300 MHz, MeOD, δ): 8.63 (dd, *J* = 4.3, 1.5 Hz, 2H), 8.20-8.33 (m, 2H), 7.70 (d, *J* = 8.0 Hz, 2H), 7.54 (d, *J* = 7.8 Hz, 1H), 7.36 (d, *J* = 8.0 Hz, 1H), 7.24-7.32 (m, 2H), 6.98-7.15 (m, 6H), 4.99 (s, 2H), 4.55 (t, *J* = 6.9 Hz, 1H), 3.14-3.30 (m, 2H), 1.42 (s, 9H). **^{13}C-NMR** (75.48 MHz, MeOD, δ): 172.8, 156.4, 150.3, 147.0, 142.6, 137.2, 136.7, 129.3, 128.8, 127.9, 127.4, 126.0, 123.2, 122.7, 121.1, 118.5, 117.9, 111.1, 109.3, 79.3, 65.9, 55.0, 53.4, 27.5. **HRMS (ESI+):** $(M+Na)^+$ calcd for $C_{36}H_{32}N_6O_4Na$, 635.2377; found: 635.2384.

*2.2.2 Synthesis of the cyclometalated iridium(III) complexes (**Ir-1, Ir-2, Ir-3**)*

The μ-dichloro cyclometalated iridium dimer intermediates were prepared by heating at reflux, in a 2-ethoxyethanol: H_2O 3:1 mixture for 24 h, $IrCl_3 \cdot xH_2O$ with either 2-phenylpyridine (ppy), 2-(2,4-

difluorophenyl)pyridine (diFppy) or 2-phenylquinoline (pq) as previously reported [8, 56]. Then, in a Schlenk tube, the suitable μ-dichloro cyclometalated iridium dimer and **L-trp** were dissolved in a methanol:dichloromethane mixture (1:1, v/v) under inert atmosphere. The vessel was sealed and the mixture heated at 50°C overnight. Upon cooling to ambient temperature, a 6-fold excess of KPF_6 was added and the suspension was let stir for 1.5 h. The insoluble salts were thus removed through filtration and the solvent concentrated under reduced pressure to obtain an oily residue. Either silica gel chromatography or precipitation were performed to achieve the desired Ir(III) complexes as pure compounds.

Ir-1. Reagents: $[Ir_2(ppy)_4(\boldsymbol{\mu}{-}Cl_2)]$ (ppy = 2-phenylpyridine; 0.09 g, 0.08 mmol), **L-trp** (0.10 g, 0.16 mmol). Solvents: dichloromethane (5 mL), methanol (5 mL). The crude product was purified through silica gel chromatography (dichloromethane: methanol 19:1, v/v) to obtain an orange solid (118 mg). **Yield:** 57%. **^{1}H-NMR** (300 MHz, $CDCl_3$, δ): 9.29 (dd, *J* = 7.9, 2.5 Hz, 2H), 9.08 (s, 1H), 8.46 (d, *J* = 8.0 Hz, 2H), 7.98 (d, *J* = 4.9 Hz, 2H), 7.92 (d, *J* = 8.1 Hz, 2H), 7.79 – 7.50 (m, 7H), 7.42 (d, *J* = 5.7 Hz, 2H), 7.36 (d, *J* = 7.8 Hz, 3H), 7.04-7.17 (m, 4H), 6.98 (t, *J* = 7.4 Hz, 2H), 6.79 (t, *J* = 6.6 Hz, 2H), 6.46 (d, *J* = 7.5 Hz, 2H), 6.29 (s, 1H), 4.96-5.19 (m, 2H), 4.74 (m, 1H), 3.27 (d, J = 4.2 Hz, 2H), 1.47 (s, 9H). **^{13}C-NMR** (75.48 MHz, $CDCl_3$, δ): 168.2, 151.8, 148.7, 145.4, 143.8, 143.1, 137.6, 132.2, 131.8, 130.6, 129.3, 127.3, 124.7, 124.4, 123.7, 122.7, 122.3, 119.3, 119.1, 28.5. **HRMS (ESI+):** $(M)^+$ calcd for $C_{58}H_{48}N_8O_4{}^{193}Ir$, 1113.3422; found: 1113.3425. **Elem. Anal.** calcd. for $C_{58}H_{48}N_8O_4{}^{193}Ir$: C, 55.50; H, 3.61; N, 8.93; found: C, 55.77; H, 3.62; N, 8.97.

Ir-2. Reagents: $[Ir_2(diFppy)_4(\boldsymbol{\mu}{-}Cl_2)]$ (diFppy = 2-(2,4-difluorophenyl)pyridine; 0.09 g, 0.07 mmol), **L-trp** (0.09 g, 0.14 mmol). Solvents: dichloromethane (8 mL), methanol (8 mL). The crude product was purified through precipitation with a mixture of dichloromethane:diethyl ether to obtain a yellow solid (60 mg). **Yield:** 31%. **^{1}H-NMR** (300 MHz, $CDCl_3$, δ): 8.32-8.48 (m, 5H), 8.21 (d, *J* = 4.9 Hz, 2H), 7.76-7.94 (m, 5H), 7.56 -7.64 (m, 2H), 7.35 (d, *J* = 5.6 Hz, 2H), 7.02-7.14 (m, 3H), 6.88-6.96 (m, 3H), 6.61-6.73 (m, 4H), 5.83 (d, *J* = 7.9 Hz, 3H), 4.97-5.28 (m, 3H), 4.81 (s, 1H),

3.20-3.41 (m, 1H), 1.50 (s, 9H). **^{19}F-NMR** (282.36 MHz, $CDCl_3$, δ): -106.52 (d, *J* = 967.4 Hz, 2F), -71.07 (d, *J* = 717.7 Hz, 2F). **^{13}C-NMR** (126 MHz, $CDCl_3$, δ): 164.9, 164.4, 162.9, 160.6, 155.2, 153.7, 148.5, 148.0, 139.1, 136.6, 128.4, 127.6, 127.5, 124.0, 123.8, 123.5, 121.7, 119.0, 118.5, 114.2, 114.1, 112.0, 99.5 (t, *J* = 27.0 Hz), 66.1, 65.7, 54.8, 53.4, 31.0, 28.4. **HRMS (ESI+):** $(M)^+$ calcd for $C_{58}H_{44}N_8F_4O_4{}^{193}Ir$, 1185.3046; found: 1185.3044. **Elem. Anal.** calcd. for $C_{58}H_{44}N_8O_4F_4{}^{193}Ir$: C, 62.13; H, 3.96; N, 9.99; found: C, 62.31; H, 3.98; N, 10.03.

Ir-3. Reagents: $[Ir_2(pq)_4(\boldsymbol{\mu}{-}Cl_2)]$ (pq = 2-phenylquinoline; 0.09 g, 0.07 mmol), **L-trp** (0.09 g, 0.14 mmol). Solvents: dichloromethane (10 mL), methanol (10 mL). The crude product was purified through precipitation with a mixture of dichloromethane:diethyl ether to obtain an orange solid (70 mg). **Yield:** 35%. **^{1}H-NMR** (300 MHz, $CDCl_3$, δ): 9.10 (d, *J* = 8.0 Hz, 1H), 8.34-8.49 (m, 2H), 8.06-8.32 (m, 8H), 7.71-7.87 (m, 2H), 7.52-7.66 (m, 4H), 6.63-7.27 (m, 20H), 4.91-5.29 (m, 3H), 4.76 (s, 1H), 3.14-3.43 (m, 1H), 1.48 (s, 9H). **^{13}C-NMR** (126 MHz, $CDCl_3$, δ): 172.3, 170.1, 155.3, 153.8, 151.4, 147.9, 145.6, 145.5, 139.9, 136.6, 135.0, 130.9, 127.4, 127.0, 124.1, 123.7, 123.1, 121.5, 119.1, 118.3, 117.4, 112.1, 108.5, 66.0, 54.7, 30.8, 28.6. **HRMS (ESI+):** $(M)^+$ calcd for $C_{66}H_{52}N_8O_4{}^{193}Ir$, 1213.3735; found: 1213.3736. **Elem. Anal.** calcd. for $C_{66}H_{52}N_8O_4{}^{193}Ir$: C, 65.33; H, 4.32; N, 9.23; found: C, 65.57; H, 4.34; N, 9.27.

2.3 Photophysical characterization

Electronic absorption spectra were obtained at room temperature in dichloromethane, by means of a Shimadzu UV3600 spectrophotometer and quartz cuvettes with 1 cm optical path length. Absolute photoluminescence quantum yields, Φ, were measured using a C11347 Quantaurus Hamamatsu Photonics K.K spectrometer, equipped with a 150 W Xenon lamp, an integrating sphere and a multichannel detector. Steady state and time-resolved fluorescence data were recorded with a FLS980 spectrofluorimeter (Edinburg Instrument Ltd). See details in Supplementary material.

2.4 Brain tissue staining and imaging

Brain tissue for this study was generated from 10–12-week-old male Sprague-Dawley rats that were excess from previous studies. Using a cryomicrotome 10 μm thick coronal cerebellum tissue sections were cut -18°C and melted onto glass microscope slides. Slides were then air dried at room temperature. Prior to staining, tissue sections were fixed in 4% formalin in phosphate-buffered saline (PBS) for 10 min and then rinsed with PBS for a further 10 min. Tissue sections were then stained with probe solution (10 μg mL-1 in DMSO, 200 μL per tissue section) and incubated for 30 min at room temperature and in the dark. Probe solution was then rinsed off with deionized water followed by rinsing with PBS for a further 10 minutes. Samples were then allowed to dry at room temperature before immediately imaging with an epifluorescence microscope (Nikon eclipse Ti2-U inverted microscope fitted with LED illumination and Nikon DS-Qi2 camera, NIS Elements standard software). Blank experiments were also prepared from serial tissue sections. A true blank was generated with no fixation or staining, and procedural blanks were generated using all reagents apart from the probe solution (instead using neat DMSO). For nuclear staining comparison, Ir-3 was counterstained with DAPI using ProLong™ Gold Antifade Mountant with DAPI (Thermo Fisher).

3. Results and discussion

3.1 Preparation of the new pro-ligand L-trp and related cyclometalated iridium(III) complexes

The new pro-ligand **L-trp** is readily prepared by reaction of 1,10-phenanthroline-5,6-dione with 4-(4-hydroxymethyl)benzaldehyde to give (4-(1H-imidazo[4,5-f][1,10]phenanthrolin-2-yl)phenyl)methanol followed by functionalization with tryptophan as shown in **Scheme 1**. Reaction of the suitable μ-dichloro cyclometalated iridium dimer with **L-trp** , followed by addition of KPF_6, affords $[Ir(ppy)_2(\mathbf{L\text{-}trp})][PF_6]$ (ppy = cyclometalated 2-phenylpyridine; **Ir-1**), $[Ir(diFppy)_2(\mathbf{L\text{-}trp})][PF_6]$ (diFppy = cyclometalated 2-(2,4-difluorophenyl)pyridine; **Ir-2**) and $[Ir(pq)_2(\mathbf{L\text{-}trp})][PF_6]$ (pq = cyclometalated 2-phenylquinoline; **Ir-3**); see details in section 2 “Materials and Methods”.

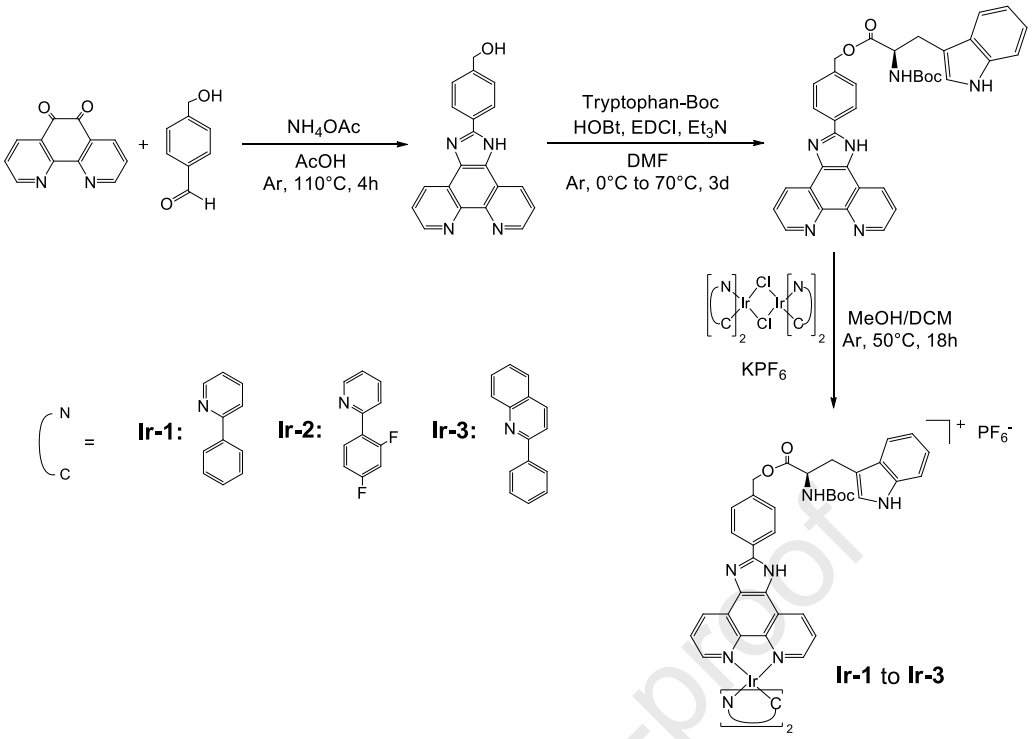

Scheme 1. Synthesis of the investigated cyclometalated iridium(III) complexes.

3.2 Photophysical properties

The absorption spectrum of the tryptophan-functionalized imidazo-phenanthroline ligand (**L-trp**) in dichloromethane solution at $1 \cdot 10^{-5}$ M is shown in Figure 1 and Figure S28. It exhibits a strong absorption in the UV region having maxima at λ = 279 and 325 nm, with an associated molar extinction coefficient (ε) of $4.2 \cdot 10^{4}$ and $2.6 \cdot 10^{4}$ M^{-1} cm^{-1}, respectively. Upon excitation at 325 nm, the **L-trp** in aerated dichloromethane solution at $1 \cdot 10^{-5}$ M gives rise to a broad emission spectrum with a maximum at λ = 408 nm (Figure S29), an absolute quantum yield (Φ_{em}) of 12 % and a measured lifetime (τ) of the excited state of 3.76 ns (Figure S30). These photophysical values are quite similar to those observed by Zhao *et al.* [53] for an analogous phenanthroline based ligand bearing a simple phenyl group instead of the benzyl 2-((*tert*-butoxycarbonyl)amino)-3-(1H-indol-3-yl)propanoate moiety.

The absorption spectra of complexes **Ir-1**, **Ir-2** and **Ir-3** dissolved in dichloromethane at $1 \cdot 10^{-5}$ M are shown in Figure 1 and relevant values are given in Table 1. All three complexes show intense absorption bands at 250–350 nm which can be attributed to π–π* ligand centered transitions (^{1}LC) from the 2-phenylpyridine to the phenanthroline moiety by analogy with related Ir(III) complexes [56-57]. As expected, weaker bands are observed at wavelengths λ > 370 nm: the low-energy absorption shoulders at ca. 380–450 nm are associated to a mixture of spin-allowed ligand-to-ligand charge transfer (^{1}LLCT) (π(ppy) → π*(phen)) and a metal-to-ligand charge-transfer (^{1}MLCT) (dπ →π*(phen)) while the transitions centered around 460 nm are attributed to a mixture of spin-forbidden metal-to-ligand charge transfer (^{3}MLCT) and ligand-to-ligand charge transfer (^{3}LLCT) transitions [56-58].

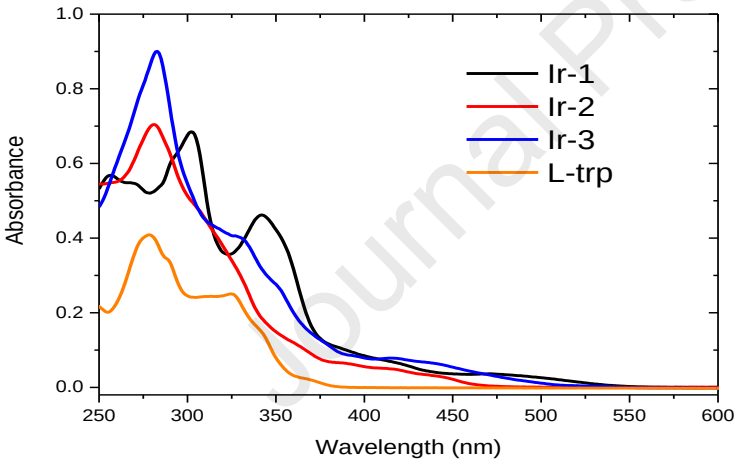

Figure 1. Absorption spectra of ligand **L-trp** and complexes **Ir-1**, **Ir-2** and **Ir-3** in dichloromethane solution at $1 \cdot 10^{-5}$ M.

Table 1. Photophysical parameters at 298 K in degassed CH_2Cl_2[a]

Complex	$\lambda_{max,abs}$ / nm [ε / $M^{-1}cm^{-1}$]	$\lambda_{max,em}$ / nm[b]	Φ_p / % degassed [aerated]	Lifetime τ	k_r / s^{-1}	k_{nr} / s^{-1}
[Ir-1]	302 [$7.1\cdot10^4$] 342 [$4.8\cdot10^4$] 474 [$3.9\cdot10^3$]	561	51.2 [5.2]	0.99 µs	$5.2\cdot10^5$	$4.9\cdot10^5$
[Ir-2]	281 [$7.2\cdot10^4$] 320 [$3.9\cdot10^4$] 413 [$5.2\cdot10^3$]	522	33.3 [6.6]	4.12 µs	$8.1\cdot10^4$	$1.6\cdot10^5$
[Ir-3]	283 [$1.0\cdot10^5$] 330 [$4.6\cdot10^4$] 414 [$8.8\cdot10^3$]	556	98.1 [43.0]	2.76 µs	$2.6\cdot10^5$	$5.3\cdot10^3$
[L-trp]	279 [$4.2\cdot10^4$][c] 325 [$2.6\cdot10^4$][c]	408[c]	12.0[c]	3.76 ns[c]	$3.2\cdot10^7$	$2.3\cdot10^8$

[a]At $2\cdot10^{-6}$ M. [b]Excitation at 400 nm. [c]At $1\cdot10^{-5}$ M.

Complexes **Ir-1**, **Ir-2** and **Ir-3** are phosphorescent in deaerated dichloromethane solution (see Figure 2) with an absolute phosphorescent quantum yield (Φ_p) and emission lifetime (τ) in the range of 33.3 – 98.1 % and 0.99 – 4.12 µs, respectively (see Table 1). The exceptional value of 98.1 % for complex **Ir-3**, similar to that reached for some neutral cyclometalated iridium(III) complexes [47], is much higher than that reported for various cationic cyclometalated iridium(III) complexes bearing a 1,10-phenanthroline based ligand [53, 56].

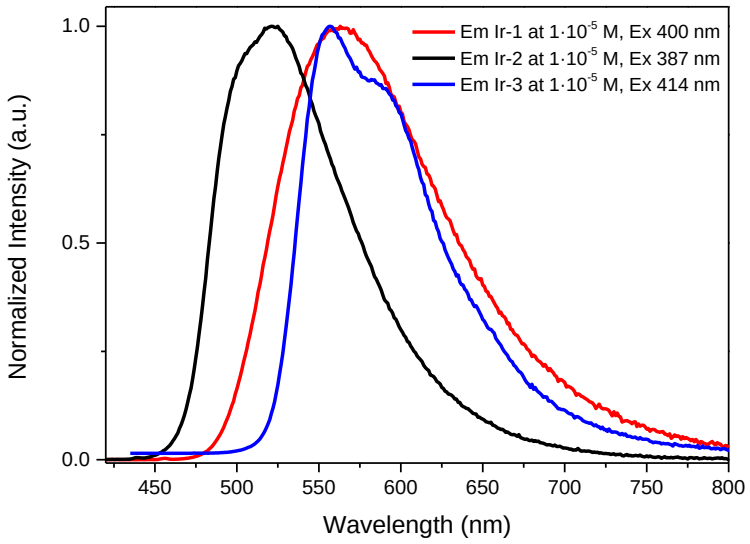

Figure 2. Emission spectra of the **Ir-1**, **Ir-2** and **Ir-3** complexes in deaerated dichloromethane solution at $1 \cdot 10^{-5}$ M, excitation wavelength around 400 nm.

According to previous works [56-57], the phosphorescence for the three complexes is attributed to a mixture of ^{3}LLCT and ^{3}MLCT transitions. It is worth pointing out that the comparison of the spectra shows a blue-shifted emission of **Ir-2** (λ_{max} = 522 nm) with respect to **Ir-1** and **Ir-3**, with maxima at 561 and 556 nm, respectively. This evidence finds explanation considering the HOMO-stabilizing effect brought about by the introduction of the fluorine atoms on the cyclometalated phenyl rings.

Usually the replacement of the phenylpyridine ligand with a phenylquinoline in Iridium(III) complexes leads to a red shift of the emission [59, 60]; nevertheless, in some cases this structural modification brings about a different behavior [61] for the proposed family of complexes, since a blue shift of the emission (from 561 nm to 556 nm) is observed, this being quite similar to previously reported phenylquinoline-Ir(III) derivatives [62]".

The radiative and non-radiative rate constants, k_r and $k_{nr,}$ for the three complexes can be determined from the phosphorescence quantum yield and the emission lifetime, according to the following equations:

$$\Phi_p = \Phi_{ISC}\left(\frac{k_r}{k_r + k_{nr}}\right)$$

$$\tau = \frac{1}{k_r + k_{nr}}$$

where Φ_{ISC} is the intersystem crossing yield (see Table 1 and Table S4). For iridium complexes, Φ_{ISC} can be assumed to be 1.0 because of the strong spin-orbit interaction caused by the heavy atom [63]; moreover, no fluorescence is detected for any complex. The calculated radiative and non-radiative rate constants are similar to those observed for other cyclometalated iridium(III) complexes bearing a 1,10-phenanthroline ligand [56].

The three complexes in dilute dichloromethane solution are efficiently quenched by oxygen: the quantum yields of **Ir-1**, **Ir-2** and **Ir-3** are 10, 5 and 2 times lower in air-equilibrated dichloromethane, respectively (Table 1). Given the efficacy of oxygen quenching, efficient production of singlet oxygen - the $^1\Delta g$ state of O_2 - can be anticipated, in agreement with previous reports on cyclometalated iridium(III) complexes as efficient photosensitizers for photodynamic therapy [12].

When the concentration of the three complexes in deaerated dichloromethane solution is increased up to $2.0 \cdot 10^{-4}$ M, a new emission band is observed at 620 and 537 nm for **Ir-1** and **Ir-2**, respectively, while no change in the emission spectrum is noted for **Ir-3** (Figure 3).

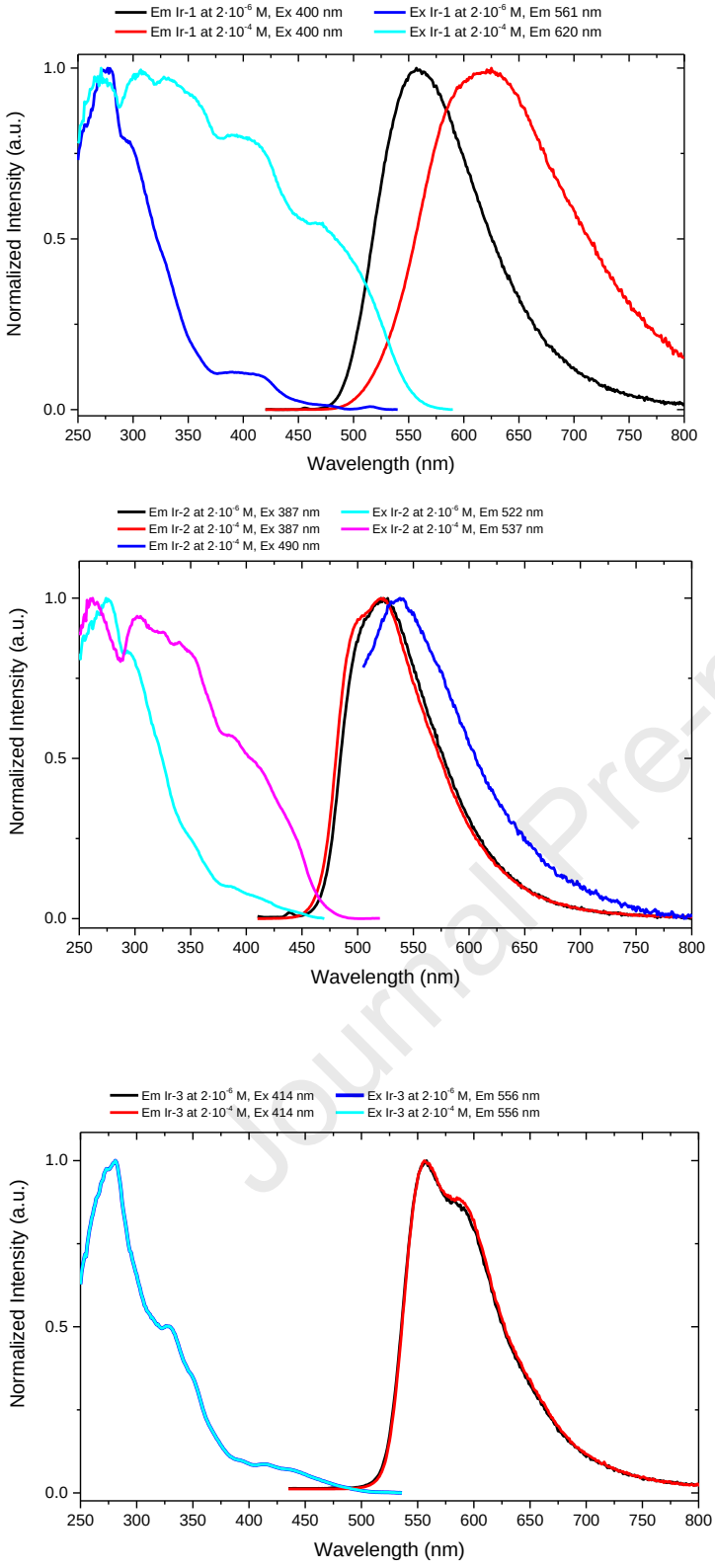

Figure 3. Emission and excitation spectra of complexes **Ir-1**, **Ir-2** and **Ir-3** in deaerated dichloromethane solution at different concentrations.

It is interesting to point out that these red shifts change by varying the excitation wavelength (Figures S8 and S16) and, in addition, the excitation spectra collected at 620 and 537 nm have a shape which is quite different with respect to those detected at lower concentration (see Figure 3). Therefore, these new emission bands of **Ir-1** and **Ir-2** can be safely ascribed to the emission from aggregate complexes rather than excimers.

As the concentration of **Ir-1**, **Ir-2** and **Ir-3** increases up to $2.0 \cdot 10^{-4}$ M, the phosphorescent quantum yield decreases reaching a value of 3.2, 3.4 and 71.4 %, respectively (see Tables S1, S2 and S3). The lifetime measurements display a bi-exponential decay for **Ir-1** and **Ir-2**, and a mono-exponential decay for **Ir-3** (see Figures S9-S10, S17-S18 and S26-S27). The observed behavior for **Ir-1** and **Ir-2** is a clear and direct consequence of the formation of aggregates, which causes a strong quenching of the emission quantum yield. Analogously, also for complex **Ir-3** it is reasonable to expect that the quenching of the quantum yield of about 27 % and the decreasing of the lifetime from 2.76 μs to 2.58 μs (Figures S21 and S26) are due to the presence of aggregates. However it should be noted that, at a concentration of $2.0 \cdot 10^{-4}$M, the emission arising from the aggregates is very weak compared to that of the **Ir-3** monomer, as also highlighted in Figure 3, in which the aggregates are not discernible.

3.3 Staining

Fluorescence microscopy reveals capability of **Ir-1**, **Ir-2** and **Ir-3** complexes to stain neuronal cells in *ex vivo* thin sections of rat cerebellum tissue (Figure 4). All three compounds displayed affinity for specific cell structures in the cerebellum tissue, with greatest image contrast observed for **Ir-3**, as seen when fluorescence images are set to a constant min-max fluorescence intensity scale (Figure 4A-C). The stronger fluorescence intensity observed for tissues stained with **Ir-3** may be the result of the stronger affinity of this compound for the tissue and/or the stronger emission intensity of this compound. Closer inspection of the images reveals affinity of **Ir-2** and **Ir-3** for axons (white matter layer indicated by σ), but not **Ir-1** (Figure 4D-F). **Ir-3** produced brightly stained soma of purkinje

and granule neurons in the cerebellum tissue (Figure 4F). In general, staining was most intense at the periphery of the granule and purkinje neurons, with visible reduced intensity toward the centre of the cell (i.e., where the nucleus is), which suggests cytoplasmic localization. At this stage the specific cell structures being stained and the molecular origin of the staining remain unknown, however staining of sub-cellular organelles within the cytoplasm such as endoplasmic reticulum, mitochondria, Golgi apparatus, lysosomes are all possibilities. Some small affinity for purkinje neurons was observed for **Ir-1** (Figure 4D), but not **Ir-2** (Figure 4E). All three compounds showed some affinity for granule neurons, which is indicated by γ symbol located to top left of neuronal cell body (Figure 4G-I), however affinity (and therefore image contrast) was greatest for **Ir-3**, which enabled simple visualization of the granule neurons (I). Panels D-I in Figure 4 have been set on individual min-max intensity scales, each optimized for maximum contrast. All compounds displayed greater fluorescence intensity in stained tissues, relative to endogenous tissue autofluorescence observed from staining with the ligand only (Figure 4J), or DMSO (Figure 4K). Panels J and K in Figure 4 are set to the same min-max intensity scale as panels A-C. The compounds could also be used in combination with DAPI nuclear stain, as shown for **Ir-3** (Figure 4L).

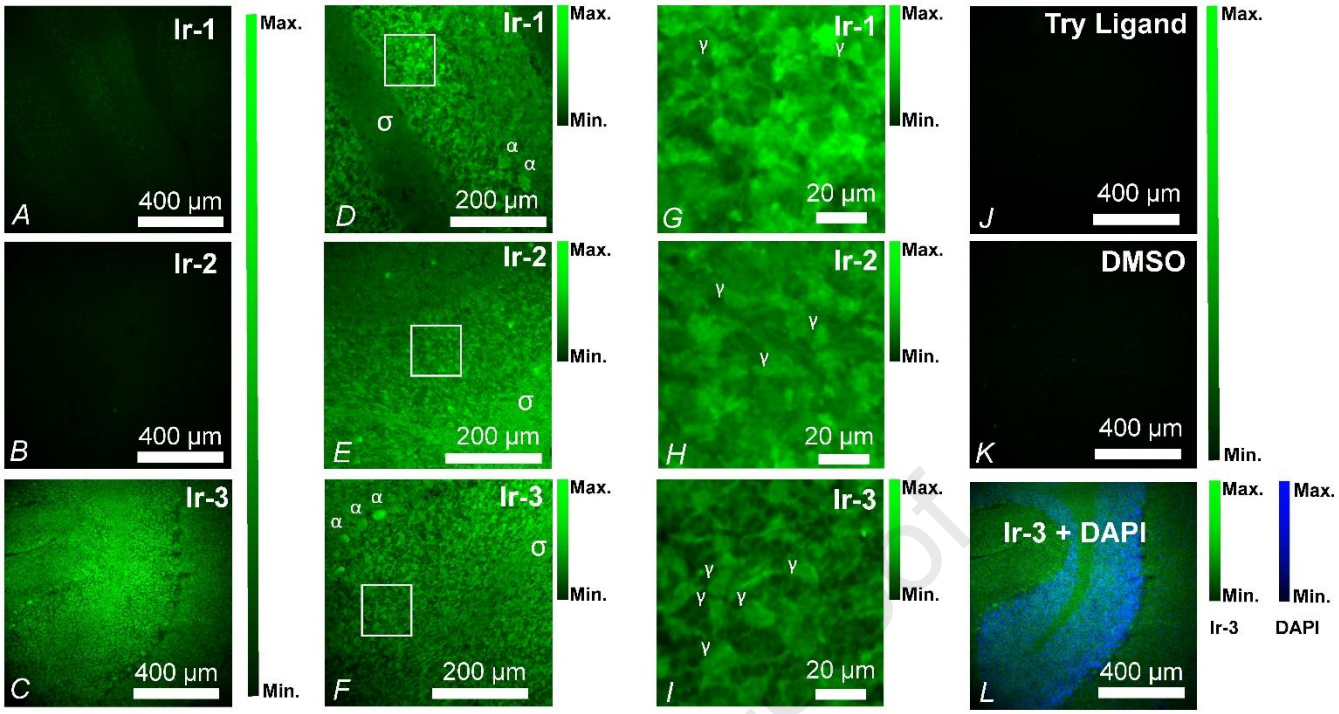

Figure 4. Fluorescence microscopy study of *ex vivo* brain tissue sections (rat cerebellum) stained with the three iridium complexes.

4. Conclusions

In conclusion, we have synthesized and well characterized three novel luminescent iridium(III) dyes functionalized with a tryptophan amino acid and bearing two cyclometalated 2-phenylpyridines (**Ir-1**), 2-(2,4-difluorophenyl)pyridines (**Ir-2**) or 2-phenylquinolines (**Ir-3**). All the complexes are able to stain neuronal cells in rat cerebellum tissue, as evidenced by fluorescence microscopy, showing affinity for granule neurons. Besides, contrarily to **Ir-1** (bearing the simple 2-phenylpyridines) both **Ir-2** and **Ir-3** also have an attraction for axons (brain white matter). The dye with two cyclometalated 2-phenylquinolines **Ir-3** is particularly fascinating, being characterized by the best luminescence quantum yield, approaching unity. Besides, it also showed a strong affinity for purkinje neurons, which constitute the output of all motor coordination in the cerebellar cortex, and it gives the greatest image contrast, producing brightly stained soma of purkinje and granule

neurons in the cerebellum tissue. Future studies will now be applied to further tissues, and also cell cultures in attempts to both further optimize staining protocols, and identify the target organelles / mode of binding.

CRediT authorship contribution statement

The manuscript was written through contributions of all authors. All authors have given approval to the final version of the manuscript.

Declaration of competing interest

The authors declare that they have no known competing financial interests or personal relationships that could have appeared to influence the work reported in this paper.

Acknowledgements

This work was supported by the National Interuniversity Consortium of Materials Science and Technology (Project INSTM21MIROBERTO), Università degli Studi di Milano (Project PSR2020_DIP_005_PI_ACOLO "Synthesis and characterization of organic and coordination compounds for application in luminescent devices or in bioimaging"), CNR and Australian Research Council (DP220103091). Fondazione Cariplo and Regione Lombardia are acknowledged for the instrumentation bought during the SmartMatLab Centre project (2014).

Appendix A. Supplementary material

Supplementary material to this article can be found online at https://doi.....

References

[1] Pawlicki M, Collins HA, Denning RG, Anderson HL. Two-photon absorption and the design of two-photon dyes. Angew. Chem. Int. Ed. 2009;48:3244-3266. doi: 10.1002/anie.200805257

[2] Edkins RM, Bettington SL, Goeta AE, Beeby A. Two-photon spectroscopy of cyclometalated iridium complexes. Dalton Trans. 2011;40:12765. doi: 10.1039/C1DT11164G

[3] Xu WJ, Liu SJ, Zhao X, Zhao N, Liu ZQ, Xu H, Liang H, Zhao Q, Yu XQ, Huang W. Synthesis, One- and Two-Photon Photophysical and Excited-State Properties, and Sensing Application of a New Phosphorescent Dinuclear Cationic Iridium(III) Complex. Chem. Eur. J. 2013;19:621. doi: 10.1002/chem.201202827

[4] Fan Y, Ding D, Zhao D. Two- and three-photon absorption and excitation phosphorescence of oligofluorene-substituted $Ir(ppy)_3$. Chem. Commun. 2015; 51:3446. doi: 10.1039/C4CC09573A

[5] Sarma M, Chatterjee T, Bodapati R, Krishnakanth KN, Hamad S, Rao SV, Das SK. Cyclometalated Iridium(III) Complexes Containing 4,4′-π-Conjugated 2,2′-Bipyridine Derivatives as the Ancillary Ligands: Synthesis, Photophysics, and Computational Studies. Inorg. Chem. 2016;55:3530-3540. doi: 10.1021/acs.inorgchem.5b02999

[6] Jin C, Liu J, Chen Y, Zeng L, Guan R, Ouyang C, Ji L, Chao H. Cyclometalated Iridium(III) Complexes as Two-Photon Phosphorescent Probes for Specific Mitochondrial Dynamics Tracking in Living Cells. Chem. Eur. J. 2015;21:12000. doi: 10.1002/chem.201501882

[7] Colombo A, Dragonetti C, Roberto D, Valore A, Ferrante C, Fortunati I, Picone AL, Todescato F, Williams JAG. Two-photon absorption properties and $^1O_2$ generation ability of Ir complexes: unexpected large cross section of [$Ir(CO)_2Cl$(4-(*para*-di-*n*-butylaminostyryl)pyridine)]. Dalton Trans. 2015;44:15712-15720. doi: 10.1039/C5DT00552C

[8] Colombo A, Garoni E, Dragonetti C, Righetto S, Roberto D, Baggi N, Escadeillas M, Guerchais V, Kamada K. A novel multifunctional cyclometallated iridium(III) complex with interesting second-order nonlinear optical properties and two-photon absorption activity. Polyhedron 2018;140:116-121. doi: 10.1016/j.poly.2017.12.009

[9] Dragonetti C, Righetto S, Roberto D, Ugo R, Valore A, Fantacci S, Sgamellotti A, De Angelis F. Cyclometallated iridium(III) complexes with substituted 1,10-phenanthrolines: a new class of highly active organometallic second order NLO-phores with excellent transparency with respect to second harmonic emission. Chem. Commun. 2007:4116-4118. doi: 10.1039/B708073E

[10] Valore A, Cariati E, Dragonetti C, Righetto S, Roberto D, Ugo R, De Angelis F, Fantacci S, Sgamellotti A, Macchioni A, Zuccaccia D. Cyclometalated Ir(III) Complexes with Substituted 1,10-Phenanthrolines: A New Class of Efficient Cationic Organometallic Second-Order NLO Chromophores Chem. Eur. J. 2010;16:4814-4825. doi: 10.1002/chem.200902788

[11] Aubert V, Ordronneau L, Escadeillas M, Williams JAG, Boucekkine A, Coulaud E, Dragonetti C, Righetto S, Roberto D, Ugo R, Valore A, Singh A, Zyss J, Ledoux-Rak I, Le Bozec H, Guerchais V. Linear and nonlinear optical properties of cationic bipyridyl iridium (III) complexes: Tunable and photoswitchable? Inorg. Chem. 2011;50:5027-5038. doi: 10.1021/ic2002892

[12] Valore A, Colombo A, Dragonetti C, Righetto S, Roberto D, Ugo R, De Angelis F, Fantacci S. Luminescent cyclometallated Ir(III) and Pt(II) complexes with β-diketonate ligands as highly active second-order NLO chromophores. Chem. Commun. 2010;46:2414–2416. doi: 10.1039/b921971d

[13] Zaarour M, Guerchais V, Le Bozec H, Dragonetti C, Righetto S, Roberto D, De Angelis F, Fantacci S, Lobello MG. An investigation on the second order nonlinear optical response of tris-cyclometallated Ir(III) complexes with variously substituted 2-phenylpyridines. Dalton Trans. 2013;42:155–159. doi: 10.1039/c2dt31839c

[14] Zaarour M, Singh A, Latouche C, Williams JAG, Ledoux-Rak I, Zyss J, Boucekkine A, Le Bozec H, Guerchais V, Dragonetti C, Colombo A, Roberto D, Valore A. Linear and Nonlinear Optical Properties of Tris-cyclometalated Phenylpyridine Ir(III) Complexes Incorporating π-Conjugated Substituents. Inorg. Chem. 52 (2013) 7987–7994. doi: 10.1021/ic400541e

[15] Dragonetti C, Colombo A, Marinotto D, Righetto S, Roberto D, Valore A, Escadeillas M, Guerchais V, Le Bozec H, Boucekkine A, Latouche C. Functionalized styryl iridium(III) complexes as active second-order NLO chromophores and building blocks for SHG polymeric films. J. Organometal. Chem. 2014;751:568-572. doi: 10.1016/j.jorganchem.2013.09.003

[16] Hierlinger C; Bradford Cordes D; Slawin A; Colombo A; Dragonetti C; Righetto S; Roberto D; Jacquemin D; Zysman-Colman E; Guerchais V. An investigation on the second-order nonlinear optical response of cationic bipyridine or phenanthroline iridium(III) complexes bearing cyclometallated 2-phenylpyridines with a triphenylamine substituent. Dalton Trans. 2018;47:8292–8300. doi: 10.1039/C8DT00754C

[17] Colombo A; Dragonetti C; Guerchais V; Hierlinger C; Zysman-Colman E; Roberto, D. A trip in the nonlinear optical properties of iridium complexes. Coord. Chem. Rev. 2020;414:213293. doi: 10.1016/j.ccr.2020.213293

[18] Iridium(III) in Optoelectronic and Photonics Applications; Zysman-Colman E Ed.; John Wiley & Sons, Inc.: Chichester, West Sussex, U.K., 2017. doi: 10.1002/9781119007166

[19] Zhu JH, Yiu SM. Tang BZ, Lo KKW. Luminescent Neutral Cyclometalated Iridium(III) Complexes Featuring a Cubic Polyhedral Oligomeric Silsesquioxane for Lipid Droplet Imaging and Photocytotoxic Applications. Inorg. Chem. 2021;60:11672-11683. doi: 10.1021/acs.inorgchem.1c01728

[20] Deaton JC, Castellano FN. Archetypal iridium(III) compounds for optoelectronic and photonic applications: photophysical properties and synthetic methods. In: Iridium(III) in optoelectronic and photonics applications. Zysman-Colman E, editor; Weinheim, Germany: Wiley-VHC; 2017 1–70 doi: 10.1002/9781119007166.ch1

[21] Evans RC, Douglas P, Winscom CJ. Coordination complexes exhibiting room-temperature phosphorescence: Evaluation of their suitability as triplet emitters in organic light emitting diodes. Coord. Chem. Rev. 2006;250:2093-2126. doi: 10.1016/j.ccr.2006.02.007

[22] Flamigni L, Barbieri A, Sabatini C, Ventura B, Barigelletti F. Photochemistry and Photophysics of Coordination Compounds: Iridium. Top. Curr. Chem. 2007;281:143-203. doi: 10.1007/128_2007_131

[23] Zhou G, Wong WY, Suo S. Recent progress and current challenges in phosphorescent white organic light-emitting diodes (WOLEDs). *J. Photochem. Photobiol. C: Photochem. Rev. 2010;11:133-156. doi: 10.1016/j.jphotochemrev.2011.01.001*

[24] Wong WY, Ho CL. Heavy metal organometallic electrophosphors derived from multi-component chromophores. *Coord. Chem. Rev. 2009;253:1709-1758. doi: 10.1016/j.ccr.2009.01.013*

[25] Zhou G, Wong WY, Yang X. New Design Tactics in OLEDs Using Functionalized 2-Phenylpyridine-Type Cyclometalates of Iridium(III) and Platinum(II). Chem. Asian J. 2011;6:1706-1727. doi: 10.1002/asia.201000928

[26] Wu H, Zhou G, Zou J, Ho CL, Wong WY, Yang W, Peng J, Cao Y. Efficient Polymer White-Light-Emitting Devices for Solid-State Lighting. Adv. Mater. 2009;21:4181-4184. doi: 10.1002/adma.200900638

[27] Chang CH, Wu ZJ, Chiu CH, Liang YH, Tsai YS, Liao JL, Chi Y, Hsieh HY, Kuo TY, Lee GH, Pan HA, Chou PT, Lin JS, Tseng MR. A New Class of Sky-Blue-Emitting Ir(III) Phosphors Assembled Using Fluorine-Free Pyridyl Pyrimidine Cyclometalates: Application toward High-

Performance Sky-Blue- and White-Emitting OLEDs. ACS Appl. Mater. Interfaces 2013;5:7341. doi: 10.1021/am401694s

[28] Slinker JD, Rivnay J, Moskowitz JS, Parker JB, Bernhard S, Abruña HD, Malliaras GG. Electroluminescent devices from ionic transition metal complexes. J. Mater. Chem. 2007;17:2976-2988. doi: 10.1039/B704017B

[29] Zysman-Colman E, Slinker JD, Parker JB, Malliaras GG, Bernhard S. Improved Turn-On Times of Light-Emitting Electrochemical Cells. Chem. Mater. 2008;20:388-396. doi: 10.1021/cm0713374

[30] Bolink HJ, Cappelli L, Coronado E, Graetzel M, Ortí E, Costa RD, Viruela M, Nazeeruddin MK. Stable Single-Layer Light-Emitting Electrochemical Cell Using 4,7-Diphenyl-1,10-phenanthroline-bis(2-phenylpyridine)iridium(III) Hexafluorophosphate. J. Am. Chem. Soc. 2006;128:14786-14787. doi: 10.1021/ja066416f

[31] Margapoti E, Shukla V, Valore A, Sharma A, Dragonetti C, Kitts C, Roberto D, Murgia M, Ugo R, Muccini M. Excimer Emission in Single Layer Electroluminescent Devices Based on [Ir(4,5-diphenyl-2-methylthiazolo)$_2$(5-methyl-1,10-phenanthroline)]$^+$ [PF$_6$]$^-$. J. Phys. Chem. C 2009;113:12517-12522. doi: 10.1021/jp901927e

[32] Wong WY, Zhou GJ, Yu XM, Kwok HS, Lin Z. Efficient Organic Light-Emitting Diodes based on Sublimable Charged Iridium Phosphorescent Emitters. Adv. Funct. Mater. 2007;17:315-323. doi: 10.1002/adfm.200600359

[33] Margapoti E, Muccini M, Sharma A, Colombo A, Dragonetti C, Roberto D, Valore A. Optoelectronic properties of OLEC devices based on phenylquinoline and phenylpyridine ionic iridium complexes. Dalton. Trans. 2012;41:9227-9231. doi: 10.1039/C2DT30800B

[34] Shavaleev NM, Scopelliti R, Graetzel M, Nazeeruddin MK, Pertegas A, Roldan-Carmona C, Torderab D, Bolink HJ. Pulsed-current versus constant-voltage light-emitting electrochemical cells with trifluoromethyl-substituted cationic iridium(III) complexes. J. Mater. Chem. C 2013;1:2241-2248.

[35] Nicewicz DA, MacMillan DWC. Merging photoredox catalysis with organocatalysis: the direct asymmetric alkylation of aldehydes. Science 2008;322:77–80. doi:10.1126/science.1161976

[36] Prier CK, Rankic DA, MacMillan DWC. Visible light photoredox catalysis with transition metal complexes: applications in organic synthesis. Chem. Rev. 2013;113:5322–63. doi:10.1021/cr300503r

[37] Fors BP, Hawker CJ. Control of a living radical polymerization of methacrylates by light. Angew. Chem. Int. Ed. 2012;51:8850–3. doi:10.1002/ anie.201203639

[38] Lalevée J, Peter M, Dumur F, Gigmes D, Blanchard N, Tehfe MA, Morlet-Savary F, Fouassier JP. Subtle ligand effects in oxidative photocatalysis with iridium complexes: application to photopolymerization. Chem. Eur. J. 2011;17: 15027–31. doi:10.1002/chem.201101445

[39] Mayo EI, Kilsa K, Tirrell T, Djurovich PI, Tamayo A, Thompson ME, Lewis NS, Gray HB. Cyclometalated iridium(III)-sensitized titanium dioxide solar cells. Photochem. Photobiol. Sci. 2006;5:871-873. doi: 10.1039/B608430C

[40] Baranoff E, Yum JH, Graetzel M, Nazeeruddin MK. Cyclometallated iridium complexes for conversion of light into electricity and electricity into light. J. Organomet. Chem. 2009;694:2661-2670. doi: 10.1016/j.jorganchem.2009.02.033

[41] Shinpuku Y, Inui F, Nakai M, Nakabayashi Y. Synthesis and characterization of novel cyclometalated iridium(III) complexes for nanocrystalline TiO_2-based dye-sensitized solar cells. J. Photochem. and Photobio. A: Chemistry 2011;222:203-209. doi: 10.1016/j.jphotochem.2011.05.023

[42] Dragonetti C, Valore A, Colombo A, Righetto S, Trafiletti V. Simple novel cyclometallated iridium complexes for potential application in dye-sensitized solar cells. Inorg. Chim. Acta 2012;388:163–167. doi: 10.1016/j.ica.2012.03.028

[43] Fiorini V, Monti N, Vigarani G, Santi G, Fasulo F, Massi M, Giorgini L, Munoz-García AB, Pavone M, Pucci A, Stagni S. Colourless luminescent solar concentrators based on Iridium(III)-Phosphors. Dyes and Pigments 2021;193:109532. doi: 10.1016/j.dyepig.2021.109532

[44] Lo KKW, Zhang KY. Iridium(III) complexes as therapeutic and bioimaging reagents for cellular applications. RSC Adv. 2012;2:12069–83. doi: 10.1039/C2RA20967E

[45] Ma S, Chen G, Xu J, Liu Y, Li G, Chen T, Li Y, James TD. Current strategies for the development of fluorescence-based molecular probes for visualizing the enzymes and proteins associated with Alzheimer's disease. Coord. Chem. Rev. 2021; 427:213553. doi: 10.1016/j.ccr.2020.213553

[46] Caporale C, Massi M. Cyclometalated Iridium(III) complexes for life science. Coord. Chem. Rev. 2018;363:71–91. doi: 10.1016/j.ccr.2018.02.006

[47] Xu K, Xie X, Zheng L-M. Iridium-lanthanide complexes: Structures, properties and applications. Coord.Chem. Rev. 2022; 456:214367. doi:1 0.1016/j.ccr.2021.214367

[48] Shaikh S, Wang Y, ur Rehman F, Jiang H, Wanga X. Phosphorescent Ir (III) complexes as cellular staining agents for biomedical molecular imaging. Coord. Chem. Rev. 2020; 416:213344.doi: 10.1016/j.ccr.2020.213344

[46] Zamora A, Vigueras G, Rodríguez V, Santana MD, Ruiz J. Cyclometalated iridium(III) luminescent complexes in therapy and phototherapy. Coord. Chem. Rev. 2018;360:34-76. doi: 10.1016/j.ccr.2018.01.010

[47] Colombo A, Fontani M, Dragonetti C, Roberto D, Williams JAG, Scotto di Perrotolo R, Casagrande F, Barozzi S, Polo S. A highly luminescent tetrahydrocurcumin Ir(III) complex with remarkable photoactivated anticancer activity. Chem. Eur. J. 2019;25:7948–7952. doi: 10.1002/chem.201901527

[48] Ho PY, Ho CL, Wong WY. Recent advances of iridium(III) metallophosphors for health-related applications. Coord. Chem. Rev. 2020;413:213267. doi: 10.1016/j.ccr.2020.213267

[49] Cho-Cheung Lee L, Lo KKW. Luminescent and Photofunctional Transition Metal Complexes: From Molecular Design to Diagnostic and Therapeutic Applications. J. Am. Chem. Soc. 2022;144:14420-14440. doi: 10.1021/jacs.2c03437.

[50] De Soricellis G, Fagnani F, Colombo A, Dragonetti C, Roberto D. Exploring the potential of N^C^N cyclometalated Pt(II) complexes bearing 1,3-di(2-pyridyl)benzene derivatives for imaging and photodynamic therapy. Inorg. Chim. Acta 2022;541:121082. doi: 10.1016/j.ica.2022.121082

[51] Xu GX, Mak ECL, Lo KKW. Photofunctional transition metal complexes as cellular probes, bioimaging reagents and phototherapeutics. Inorg. Chem. Frontiers. 2021;8:4553-4579. doi: 10.1039/d1qi00931a.

[52] Lo KKW. Molecular Design of Bioorthogonal Probes and Imaging Reagents Derived from Photofunctional Transition Metal Complexes. Acc. Chem. Res. 2020;53:32-44. doi: 10.1021/acs.accounts.9b00416.

[53] Sun J, Wu W, Guo H, Zhao J. Visible-Light Harvesting with Cyclometalated Iridium(III) Complexes Having Long-Lived 3IL Excited States and Their Application in Triplet–Triplet-Annihilation Based Upconversion. Eur. J. Inorg. Chem. 2011;21:3165-3173. doi: 10.1002/ejic.201100501

[54] Wolf H. The effect of hormones and vitamin B6 on urinary excretion of metabolites of the kynurenine pathway. Scand. J. Clin. Lab. Invest. Suppl. 1974;136:1-186.

[55] Pardridge WM. Blood-Brain Barrier Carrier-Mediated Transport and Brain Metabolism of Amino Acids. Neurochem. Res. 1998;23:635-644. doi: 10.1023/A:1022482604276

[56] Dragonetti C, Falciola L, Mussini P, Righetto S, Roberto D, Ugo R, Valore A, De Angelis F, Fantacci S, Sgamellotti A, Ramon M, Muccini M. The Role of Substituents on Functionalized 1,10-Phenanthroline in Controlling the Emission Properties of Cationic Iridium(III) Complexes of Interest for Electroluminescent Devices Inorg. Chem. 2007;46:8533–8547. doi: 10.1021/ic700414z15

[57] Mandal S, Poria DK, Ghosh R, Ray PS, Gupta P. Development of a cyclometalated iridium complex with specific intramolecular hydrogen-bonding that acts as a fluorescent marker for the endoplasmic reticulum and causes photoinduced cell death. Dalton Trans. 2014;43:17463-17474. doi: 10.1039/C4DT00845F

[58] Ladouceur S, Zysman-Colman E. A Comprehensive Survey of Cationic Iridium(III) Complexes Bearing Nontraditional Ligand Chelation Motifs. Eur. J. Inorg. Chem.;2013 2985. doi: 10.1002/ejic.201390073

[59] Lamansky S, Djurovich P, Murphy D, Abdel-Razzaq F, Lee H-E, Adachi C, Burrows P E, Forrest S R, Thompson E T. Highly Phosphorescent Bis-Cyclometalated Iridium Complexes: Synthesis, Photophysical Characterization, and Use in Organic Light Emitting Diodes. J. Am. Chem. Soc.; 2001;123:4304-4312. doi: 10.1021/ja003693s

[60] Kim DH, Cho NS, Oh H-Y , Yang JH , Jeon WS, Jung Park J S, Suh M C , Kwon JH. Highly Efficient Red Phosphorescent Dopants in Organic Light-Emitting Devices. Adv. Mater. 2011;23: 2721–2726 doi: 10.1002/adma.201100405.

[61] Nam JS, Kang M-G, Kang J, Park S-Y, Lee SJC, Kim H-T, Seo JK, Kwon O-H, Lim MH, Rhee H-W, Kwon T-H. Endoplasmic Reticulum-Localized Iridium(III) Complexes as Efficient Photodynamic Therapy Agents via Protein Modifications J. Am. Chem. Soc. 2016;138:10968−10977 doi:10.1021/jacs.6b05302

[62] Liu B, Lystrom L, Brown SL, Hobbie EK, Kilina S, Sun W. Impact of Benzannulation Site at the Diimine (N^N) Ligand on the Excited-State Properties and Reverse Saturable Absorption of Biscyclometalated Iridium(III) Complexes. Inorg. Chem. 2019; 58:5483−5493. doi: 10.1021/acs.inorgchem.8b03162.

[63] Cummings SD, Eisenberg R. Tuning the Excited-State Properties of Platinum(II) Diimine Dithiolate Complexes. J. Am. Chem. Soc. 1996;118:1949-1960. doi: 10.1021/ja951345y

Highlights

- Luminescent cyclometalated iridium(III) dyes with a tryptophan amino acid
- Dyes able to stain neuronal cells in rat cerebellum tissue
- Strong affinity for purkinje neurons in cerebellum tissue

Declaration of interests

☒ The authors declare that they have no known competing financial interests or personal relationships that could have appeared to influence the work reported in this paper.

☐ The authors declare the following financial interests/personal relationships which may be considered as potential competing interests: